The Two-Dimensional Hydrogen Atom

A Thesis
Presented to
The Division of Mathematics and Natural Sciences
Reed College

In Partial Fulfillment
of the Requirements for the Degree
Bachelor of Arts

Todd S. Garon

May 2011

Approved for the Division
(Physics)

_____

Nelia Mann

Acknowledgements

I would like to thank a few people[1]: the Paradox, Dylan, Max & Sid, Jess & Farren, my parents, David Griffiths, Joel Franklin, and especially my lovely thesis advisor Nelia Mann.

Thank you all so much, I couldn't have done this without you.

[1] this list is by no means exhaustive

Table of Contents

List of Tables

List of Figures

Abstract

The two dimensional hydrogen atom has been extensively studied using variational methods by Asturias and Aragón [1] and Reiser [2]. Using a simple numerical method implemented by Franklin and Garon [3] we can very quickly probe the spectrum of the two dimensional hydrogen atom to an extremely high accuracy and use this method to find the energy of the system as a function of the angular momentum and principal quantum numbers, finding excellent agreement with Asturias and Aragón [1] and Reiser [2]. We extend these results in an attempt to find an arbitrary dimensional expression using the logarithmic potential and into an exploration of the relativistic spectrum of the two dimensional hydrogen atom.

Introduction

This thesis asks a simple question: what is the spectrum of hydrogen in two spatial dimensions?

To begin, we need to define a few terms, starting with what is meant by two dimensions. We could be in a higher dimensional space and somehow confine our system to two dimensions through electromagnetic interactions or other such effects; alternatively we could actually be in a two dimensional space. Both cases will be analyzed and they produce very different results, but we will focus on the second because it is the more interesting case.

By hydrogen, we mean a system in which we have a moving electron of charge $-e$ "orbiting" a stationary proton of charge e. There is some electromagnetic interaction between the proton and the electron. We will ignore other effects except when noted.

Before we jump in there is one final caveat: the word "dimension" will be used to mean three things. For constants, we use it to mean a quantity's unit of measurement like mass or length; for matrices, we use it to mean their size; finally, and most often, we use it to mean the number of coordinates that we need to uniquely define a point in a space. For two dimensional space, we need two values to define any point.

We start by looking at potentials and semi-classical models, moving on to non-relativistic and finally relativistic quantum mechanical models of the two dimensional hydrogen atom.

0.1 Hydrogen in Three or More Dimenions

In three dimensions the potential energy of our system is described by the familiar Coulomb potential

$$V(r) = -\frac{e^2}{4\pi\epsilon_0}\frac{1}{r}. \tag{1}$$

The bound-state energies of the system can be found by solving the time independent Schrödinger equation,

$$E\psi = -\frac{\hbar^2}{2m}\nabla^2\psi + V(r)\psi. \tag{2}$$

This can be solved by writing the Laplacian, ∇^2, in spherical coordinates and applying separation of variables to obtain a purely radial equation

$$ER(r) = -\frac{\hbar^2}{2m}\frac{1}{r^2}\frac{d}{dr}\left(r^2\frac{d}{dr}R(r)\right) + \left(\frac{\hbar^2}{2m}\frac{\ell(\ell+1)}{r^2} + V(r)\right)R(r), \tag{3}$$

where ℓ is the quantized orbital angular momentum and $\ell(\ell+1)$ are the eigenvalues of the L^2 operator. Using a standard series solution we can find the spectrum

$$E_n = -\frac{\alpha^2 mc^2}{2n^2}, \tag{4}$$

where $\alpha = \frac{e^2}{4\pi\epsilon_0\hbar c}$ is the fine structure constant and n is the principal quantum number [4].

Suppose we consider confining our electron to a plane containing the proton. In this system, our potential does not change, since we have only artificially constrained the particle to two dimensions. The Schrödinger equation itself is invariant to this change but its components, the Laplacian ∇^2 and the eigenvalues of L^2, are not. The eigenvalues of L^2 become ℓ^2 for reasons that will be explained later in section 1.1. With the appropriate modifications, our radial equation becomes

$$ER(r) = -\frac{\hbar^2}{2m}\frac{1}{r}\frac{d}{dr}\left(r\frac{d}{dr}R(r)\right) + \left(\frac{\hbar^2}{2m}\frac{\ell^2}{r^2} + V(r)\right)R(r) \tag{5}$$

with energies [5]

$$E_n = -\frac{\alpha^2 mc^2}{2(n-1/2)^2}. \tag{6}$$

It is important to notice that the two and three dimensional Coulomb solutions look very similar. In the large n limit they converge because the $1/2$ term in Eqn (6) becomes negligible. In the small n limit we expect our energies to be lower in two dimensions than in three. In addition, both systems are degenerate in ℓ.[2]

The trouble with this solution is that it leaves an important point unaddressed: our potential is inherently three dimensional. It is the result of using Gauss' law,

$$\oint \vec{E}\cdot d\vec{a} = \frac{q_{enc}}{\epsilon_0} \tag{7}$$

with a spherical Gaussian surface. There is an assumption that a third spatial dimension must exist and therefore this model really is not two dimensional.

In a four dimensional space we can find a potential from Gauss' Law proportional to $1/r^2$ and as a result find a continuous spectrum without a ground state [6]. Higher dimensional spaces have potentials proportional to $1/r^{D-2}$ and have spectra in two spatial dimensions [7].

[2]The constraint to two dimensions does not break the symmetry of the Runge-Lenz vector, conserving the degeneracy in ℓ.

0.2 The Attractive Potential in Two Dimensions

Given that any higher dimensional model constrained to two dimensions is not actually two dimensional, we must look for a potential that is truly two dimensional in order to reflect the physical limitation of the space. We take as an assumption that classical electromagnetism is otherwise unmodified in one less spatial dimension.

In a two dimensional world a point charge with charge e can be enclosed by a circle of radius r, as shown in Figure 1. Using Eqn (7) we find that the electric field is

$$\vec{E}(r) = \frac{e}{2\pi\tilde{\epsilon}_0 r}\hat{r} \tag{8}$$

where $\tilde{\epsilon}_0$ is the value of ϵ_0 in two dimensions. If we take a look at the dimension of our solution we can see that the dimensions of $\tilde{\epsilon}_0$ are not the same as ϵ_0. We would like to keep the value and dimension of our constants the same between the two and three dimensional cases for ease of comparison between them. A solution is to let $\tilde{\epsilon}_0 = \xi\epsilon_0$ where ξ is a constant with dimension of length. This makes our electric field

$$\vec{E}(r) = \frac{e}{2\pi\epsilon_0\xi r}\hat{r} \tag{9}$$

which is analogous to that of an infinite wire in (3+1) dimensions of linear charge density e/ξ.

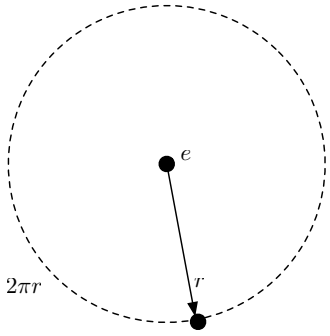

Figure 1: A plot of the Gaussian surface enclosing a point charge in (2+1) dimensions.

Invoking the relationship between electric potential $\tilde{V}$ and field $\vec{E} = -\vec{\nabla}\tilde{V}$, we find that our electric potential is

$$\tilde{V}(r) = \frac{-e}{2\pi\epsilon_0\xi}\int_{r_0}^{r}\frac{1}{\tilde{r}}d\tilde{r}. \tag{10}$$

We measure the potential from a finite reference point r_0 because the the logarithm is infinite at spatial infinity. The potential energy $V(r)$ of the electron is

$$V(r) = \frac{e^2}{2\pi\epsilon_0\xi}\log\left(\frac{r}{r_0}\right). \tag{11}$$

Figure 2 is a plot of this potential. This potential ranges from $-\infty$ to ∞, with a zero set by the length scale r_0, whereas the Coulomb potential asymptotically goes to zero as $r \to \infty$. One interesting observation is that due to the range of the logarithmic potential there can be no scattering states – every state is a bound state. Since there will be no scattering states, we also expect that some bound states will have positive energy.

This potential also has two length scales, ξ and r_0. We can think of r_0 as defining the zero of the potential but otherwise it has no physical significance, whereas ξ is an intrinsic fundamental length scale in two dimensions. We have no intuition into what this length scale is, but if we package $\frac{e^2}{2\pi\epsilon_0\xi}$ into an energy scale Ω we will have have fewer moving parts. This gives us

$$V(r) = \Omega \log\left(\frac{r}{r_0}\right). \tag{12}$$

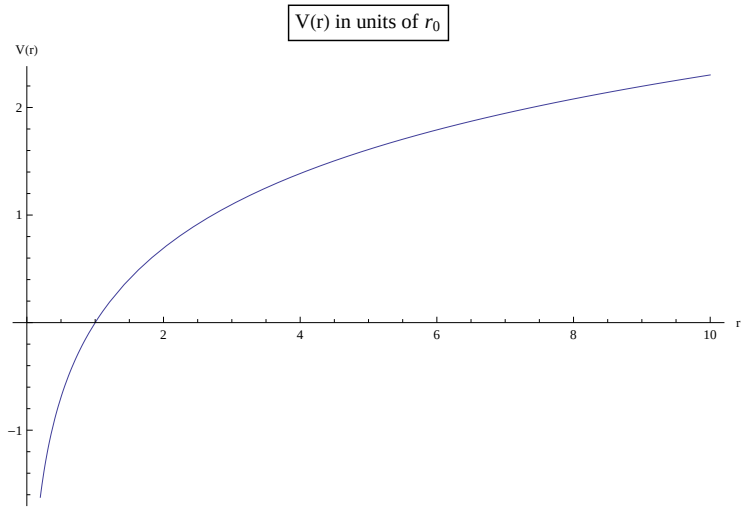

Figure 2: A plot of the logarithmic potential in units of r_0.

0.3 The Bohr Model

Since we now have a potential, we should begin to think about how to find the spectrum of our system. One simple semi-classical tool we should try is the Bohr model. Despite its physically dubious assumptions, it produces enlightening results.

The Bohr model makes three assumptions: we can write down the Hamiltonian, the electron moves in circular orbits around the proton,[3] and the classical angular

[3]A generalization, the Sommerfeld model, allows the particle to move in noncircular orbits and it gives some idea of our system's dependence on ℓ. We go through the derivation of the Sommerfeld model and solve it for the logarithmic potential in Appendix A.

momentum is quantized by the equation $L = \hbar n$ for integer n [8]. The last is the only quantum condition in the classical model. The Bohr model also requires that $D \geq 2$ but does not depend on dimension beyond this. We can fulfill the first condition by writing down the most general Hamiltonian with a central potential

$$H = \frac{p^2}{2m} + V(r), \tag{13}$$

where p is the momentum and m is the mass of the electron. We would like to find the radius of circular orbits, where the centripetal force is equal to the force from the potential, $\vec{F} = -\vec{\nabla}V$. This is equivalent to the condition $\frac{\partial H}{\partial r} = 0$. Rewriting the momentum p in terms of the angular momentum L, $p = L/r$, this derivative condition can be expressed as

$$0 = -\frac{L^2}{mr^3} + \frac{\partial V}{\partial r}. \tag{14}$$

For a given potential we can solve for r, impose the quantization condition, and plug this result back into the Hamiltonian to give us a quantization of the energy levels. If we were to use the Coulomb potential, we would find the correct spectrum for hydrogen.

We need to recognize the caveats of this model. It is oblivious to other quantum numbers. This may be obvious since there is no term dependent on them in the Hamiltonian, but we are given no knowledge of what effect other quantum numbers such as the orbital angular momentum quantum number ℓ will have on the spectrum. This is not problematic for the Coulomb potential because of its degeneracy. The Bohr model also tends to incorrectly place the ground state. For example, for the three-dimensional harmonic oscillator the Bohr model predicts that the energy levels should be $E_n = \hbar\omega n$ while the actual energy levels are $\hbar\omega(n + 3/2)$ for $n \in \mathbb{Z}_{>0}$. It is also non-relativistic and insensitive to a change in the number of dimensions without a change in the potential. Given these potentially sizable caveats, it can still be a useful tool in understanding the spectrum of two dimensional hydrogen.

Letting $\bar{H} = H/\Omega$, the Bohr Hamiltonian for our system is

$$\bar{H} = \frac{L^2}{2m\Omega r^2} + \log(r/r_0). \tag{15}$$

The radius of circular orbits is

$$r_{\text{circ}} = \sqrt{\frac{L^2}{\Omega m}}. \tag{16}$$

Plugging $r_{\min}$ into the Hamiltonian, and setting $r_0 = \frac{\hbar}{\sqrt{2\Omega m}}$,[4] the Bohr spectrum with the logarithmic potential is

$$\bar{E}_n = \frac{1 + \log 2}{2} + \log n. \tag{17}$$

[4]This definition will be motivated later.

We should observe that the spectrum has an infinite number of positive energy bound states, as expected. If we chose a different value of r_0, we would shift the entire spectrum up or down; with this choice of r_0 the entire spectrum is positive.

Given the caveats about the Bohr model from earlier, Eqn (17) may not accurately reflect the spectrum, so we need to attack the problem differently. We can still use this result to inform our knowledge of solutions using more labor intensive methods. We will guess that our solution may be of the general form

$$E_n = A + \log(n + C). \tag{18}$$

To find a better solution, we need to solve the Schrödinger equation with our logarithmic potential.

0.4 The Relativistic Bohr Model

We are also interested in studying what occurs when relativistic effects are taken into account, and we can create a Bohr model to give us some insight. In the non-relativistic model we use the non-relativistic kinetic energy, so very reasonably the relativistic Bohr model should use the expression for relativistic kinetic energy. With this substitution the Hamiltonian is

$$H = \sqrt{p^2c^2 + m^2c^4} + V(r). \tag{19}$$

This model works in the same way as the non-relativistic Bohr model. For the $1/r$ potential, the spectrum from this model is

$$E_n = mc^2\sqrt{1 - \frac{\alpha^2}{n^2}}. \tag{20}$$

This is the relativistic spectrum for hydrogen with zero orbital angular momentum [9]. The relativistic treatment of angular momentum is different from the non-relativistic treatment insofar as we work with the total angular momentum, which for this system is the orbital angular momentum ℓ and the contribution from the spin of the electron $\pm 1/2$. If it were not for the degeneracy of our system we would expect to get a mixing of states from both possible values of ℓ. The Bohr model is oblivious to ℓ and so it will not reproduce this effect. We can also expand this to first order in α^2 and find that we get back the rest energy of the election plus the non-relativistic spectrum.

This procedure also works for the logarithmic potential. Letting $\nu = mc^2/\Omega$ and $\omega = \frac{L^2}{m^2c^2}$, the Hamiltonian becomes

$$\bar{H} = \nu\sqrt{\frac{\omega}{r^2} + 1} + \log r/r_0. \tag{21}$$

The radius of circular orbits can be found from setting $\frac{\partial \bar{H}}{\partial r} = 0$,

$$r = \sqrt{\frac{\omega}{2}\left(-1 + \sqrt{4\nu^2 + 1}\right)}. \tag{22}$$

Plugging this radius back into the Hamiltonian, the spectrum is

$$\bar{E}_n = P(\nu) + \frac{1+\log 2}{2} + \log n \tag{23}$$

where

$$P(\nu) = \nu\sqrt{\frac{2}{-1+\sqrt{4\nu^2+1}}+1} + \frac{1}{2}\log\left(\frac{-1+\sqrt{4\nu^2+1}}{2\nu}\right) - \frac{1}{2}. \tag{24}$$

Figure 3 is a plot of $P(\nu) - \nu$.

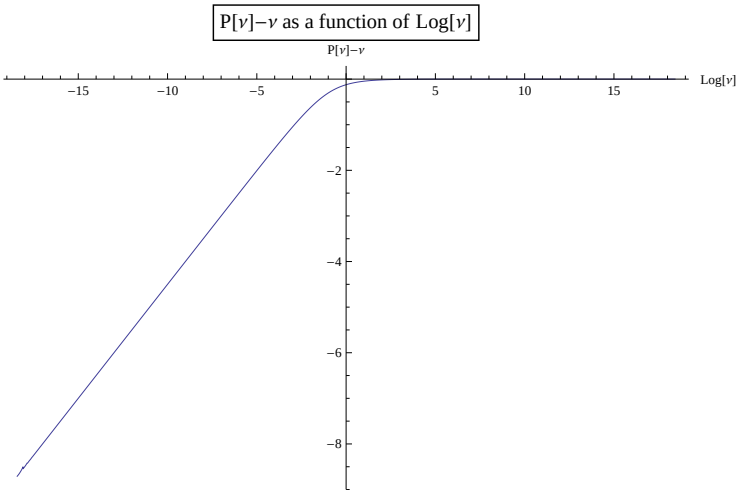

Figure 3: A plot of $P(\nu) - v$ as a function of $\log \nu$. We can see that this function is zero for large ν and linear for small ν.

In the large ν limit, $\bar{E}_n$ is

$$\bar{E}_n \approx \nu + \frac{1+\log 2}{2} + \log n. \tag{25}$$

Not surprisingly, we get back what we should expect when our system is non-relativistic: the non-relativistic spectrum plus ν. We should also look at the small ν limit, $\nu \ll 1$,

$$\bar{E}_n \approx \frac{1+\log(\nu)}{2} + \frac{1+\log 2}{2} + \log n. \tag{26}$$

In the small ν regime, we find a spectrum that is the non-relativistic spectrum plus an offset proportional to $1+\log\nu$. In between these limits, we obtain a more complicated ν dependent offset. From the relativistic Bohr model we can expect a spectrum of the form

$$\bar{E}_\nu = A(\nu) + \log(n + C(\nu)). \tag{27}$$

Chapter 1

The (2+1) Hydrogen Spectrum

In attacking the spectrum of the hydrogen atom in (2+1) dimensions we are about to be faced with a litany of new and interesting technicalities. The analytic and perturbative techniques that carry one through undergraduate physics become useless. We are instead faced with a numerical problem where the solution must be interpreted, where one must separate the errors necessarily present from the physics.

1.1 The Schrödinger treatment

To find the non-relativistic spectrum we need the time-independent form of the Schrödinger equation pertinent to our system. This will be

$$E\psi(r,\theta) = \frac{-\hbar^2}{2m}\nabla^2\psi(r,\theta) + \Omega\log\left(\frac{r}{r_0}\right)\psi(r,\theta), \tag{1.1}$$

where

$$\nabla^2\psi = \frac{1}{r}\frac{\partial}{\partial r}\left(r\frac{\partial\psi}{\partial r}\right) + \frac{1}{r^2}\frac{\partial^2\psi}{\partial\theta^2}. \tag{1.2}$$

Trying a separable solution, $\psi(r,\theta) = R(r)\Theta(\theta)$, our equation becomes

$$\frac{2mr^2}{\hbar^2}\left(E - \Omega\log\left(\frac{r}{r_0}\right) + \frac{\hbar^2}{2m}\frac{1}{rR}\frac{d}{dr}\left(r\frac{dR}{dr}\right)\right) = -\frac{1}{\Theta}\frac{d^2\Theta}{d\theta^2}. \tag{1.3}$$

We know that the portion dependent on θ must be equal to a constant; we will call it $-\ell^2$, so we have

$$\frac{2mr^2}{\hbar^2}\left(E - \Omega\log\left(\frac{r}{r_0}\right) + \frac{\hbar^2}{2m}\frac{1}{rR}\frac{d}{dr}\left(r\frac{dR}{dr}\right)\right) = \ell^2. \tag{1.4}$$

We can solve the angular equation

$$-\ell^2 = \frac{1}{\Theta}\frac{d^2\Theta}{d\theta^2} \tag{1.5}$$

to find that the solution is

$$\Theta(\theta) = Ae^{i\ell\theta} + Be^{-i\ell\theta}, \tag{1.6}$$

with $\ell \in \mathbb{Z}$ required for periodicity. The remaining radial component is

$$ER(r) = \frac{-\hbar^2}{2m}\left(R''(r) + \frac{1}{r}R'(r)\right) + \left(\frac{\hbar^2}{2m}\frac{\ell^2}{r^2} + \Omega \log\left(\frac{r}{r_0}\right)\right) R(r). \tag{1.7}$$

A natural step to solving this equation is to nondimensionalize it, replacing our fundamental constants with dimensionless constants. The reason for this is twofold: we get to write down a simpler equation, one that may only involve two or three constants which represent fundamental length and energy scales for our problem, and this equation can easily be converted into something we can approach with numerical methods.

To do this let $r = \rho_0\rho$ where ρ is a dimensionless quantity. Plugging the new definition of r into the radial equation, we find that

$$\frac{2mE\rho_0^2}{\hbar^2}R = -\frac{1}{\rho}\frac{dR}{d\rho} - \frac{d^2R}{d\rho^2} + \left(\frac{\ell^2}{\rho^2} + \frac{2\Omega m\rho_0^2}{\hbar^2}\log(\rho_0\rho/r_0)\right) R. \tag{1.8}$$

Since ρ_0 is an undefined length scale we can pick its value such that it simplifies the equation. Such a definition is to let $\rho_0^2 = \frac{\hbar^2}{2\Omega m}$. If we also define $\bar{E} = \frac{E}{\Omega}$ and set $\rho_0 = r_0$ our equation becomes

$$\bar{E}R = -\frac{1}{\rho}\frac{dR}{d\rho} - \frac{d^2R}{d\rho^2} + \left(\frac{\ell^2}{\rho^2} + \log(\rho)\right) R. \tag{1.9}$$

Recall that we can set r_0 as we like because any definition only shifts the spectrum. This definition is consistent with our choice for the Bohr spectrum.

There are a few immediate ways that we should think of using to solve this equation: series solutions, using limiting cases, and perturbative approaches. If we were to try a series solution we would be bogged down by being unable to Taylor expand the logarithm near 0 where we would naturally like to do so. The wave function should be localized for small n and ℓ near 0, so the inability to simplify the potential by only keeping the lower order, hopefully tractable, terms of the expansion is problematic. We could try Taylor expanding in the area around the zero of the potential, at $\rho = 1$. However this leaves us to solve two differential equations, for the wave function on the left and right of 1 separately, stitch them together using continuity, and then solve the eigenvalue problem again. This might work if we knew how many terms of the infinite series we need to keep for the approximation of the potential to be accurate over the entire range of the wave function, but we have no such intuition. We could also look at limits of the differential equation and build up an ansatz for the full solution from that. This is usually a useful idea but the potential goes to $\pm\infty$ at the two points, 0 and ∞, where we would normally try this technique. In particular it is not the range of potential that causes this to fail but how it scales which creates issues.

A perturbative approach would be to engineer a soluble potential that approximates the logarithmic potential, solve, and use the properties of the solution to put upper bounds on the spectrum though variational methods. This was used in [1] by applying a variational method to Eqn (1.9) using the wave functions of the two dimensional harmonic oscillator and then numerically minimizing the energies [1, 10, 2]. However, it is computationally expensive and does not probe what the values actually are, which is what we should be after. Instead, we will apply a "finite difference method" to Eqn (1.9). Note that the exact form of Eqn (1.9) agrees with the equation explored in [1], allowing us to compare our results directly to theirs.

1.2 Finite Difference Methods

Since our usual analytic and perturbative tools are ineffective or difficult to apply we need to move to numerical approximations. A natural approach is to use a finite difference method which maps our problem into a finite eigenvalue problem [3]. This method replaces our infinite dimensional operators with discrete approximations to them.

Given a second order differential equation, we discretize the equation by placing it on a finite spatial grid of N points: we use a regular grid spacing $\Delta\rho$, where $\rho_i = i\Delta\rho$ for $i \in 1, 2, \ldots, N$. To place the equation on the grid we need to find an approximation to the first and second derivatives. We know that we can express the derivative as the difference between two points divided by the space between them. We can make this heuristic notion concrete by taking the difference of two Taylor expansions, one at $R(\rho_j + \Delta\rho)$ and the other at $R(\rho_j - \Delta\rho)$

$$R'(\rho_j) = \frac{R(\rho_j + \Delta\rho) - R(\rho_j - \Delta\rho)}{2\Delta\rho} + O(\Delta\rho^2). \tag{1.10}$$

Using the same two Taylor expansions, we can take their sum and find an approximation to the second derivative

$$R''(\rho_j) = \frac{R(\rho_j + \Delta\rho) - 2R(\rho_j) + R(\rho_j - \Delta\rho)}{\Delta\rho^2} + O(\Delta\rho^2). \tag{1.11}$$

When we apply this set of approximations to a differential equation at each grid point, we create a matrix that approximates the value of the differential operator. This system can be thought of as

$$\bar{E}\vec{R} = \mathbb{D}\vec{R}. \tag{1.12}$$

where $\mathbb{D}$ is a matrix representing the discretized Hamiltonian operator and $\vec{R}$ is a vector with elements $R_j = R(\rho_j)$. We can solve for $\bar{E}$ using any sort of eigenvalue routine that takes advantage of $\mathbb{D}$'s sparsity and is efficient at finding relatively few eigenvalues[1].

[1] $\mathbb{D}$ is tridiagonal and, for reasons we will describe later, huge. To find the eigenvalues we use Mathematica's function for Lanczos iteration in its ARPACK implementation. See Golub and Van Loan [11] or Saad [12] for more information.

We must also consider what to do at the boundaries. Our approximations to the first and second derivative ask for the value of R_0 when we want to approximate R_1. We know from (3+1) dimensional hydrogen that the wave function is either 0 or finite for $\ell \neq 0$. It seems prudent to set $R_0 = 0$. For $\ell = 0$ this leaves us with a boundary condition mismatch that is potentially problematic. On the other end, the wave functions are normalized, so they should decay to zero, meaning R_{N+1} should be zero.

We can cook up a change of variables such that we fulfill the boundary conditions of the numerical method. Letting $u = \sqrt{\rho}R$, our initial differential equation Eq (1.9) becomes [2]

$$\bar{E}u = -u'' + \left(\frac{\ell^2 - 1/4}{\rho^2} + \log(\rho)\right) u. \tag{1.13}$$

For $\ell = 0$ we would like to force our wave functions to go to zero faster to ensure we match our boundary conditions and have a normalizable wave function. Using the change of variables $u = \rho R$, we find that our differential equation is now

$$-u'' + \frac{u'}{\rho} + \left(\frac{\ell^2 - 1}{\rho^2} + \log\rho\right) u = \bar{E}u. \tag{1.14}$$

These two changes of variables both ensure that $u_0 = 0$ and $u_{N+1} = 0$ are appropriate boundary conditions. The energies are unchanged. We use Eqn (1.13) for $\ell \neq 0$ and Eqn (1.14) for $\ell = 0$.

Finally, our wave functions are approximated on a grid of N points that goes all the way out to ∞. We need to rein in our grid somehow since ∞ is hard to model on a computer. To get around this we can arbitrarily choose some point, ρ_∞, where $u(\rho_\infty) \approx 0$. It is natural to define $\Delta\rho = \frac{\rho_\infty}{N}$ to insure a uniform grid spacing.

In previous work we have have shown that this method recreates the energy eigenvalues for (3+1) relativistic and non-relativistic hydrogen and can handle difficult potentials like that from Born-Infeld electrodynamics [3].

1.3 Data

Before we go about finding the eigenvalues of large sparse matrices we need to set the two free parameters, ρ_∞ and N, in our discretization. We can choose ρ_∞ by looking at the eigenvalues for states with large ℓ and n for various ρ_∞ and finding a value such that the wave functions have essentially decayed to zero within this bound. We choose N by increasing it until our eigenvalues for small n and ℓ have converged to some specified accuracy. Through such a process we found that these values are $\rho_\infty = 400$ and $N = 100000$, giving a $\Delta\rho = 1/250$.

Now we need to find a proper scaling for ρ_∞ with ℓ, which we can do by looking

[2] A side effect of the change of variables is manifest in that we get equivalent values at $N = 10^6$ using a discretized Eqn (1.9) as we do at $N = 10^5$ using Eqn (1.13).

at the effective potential[3]

$$V_{\text{eff}} = \frac{\ell^2}{\rho^2} + \log \rho. \tag{1.15}$$

The minimum of the effective potential should have some ℓ dependence and it is

$$\rho_{\min} = \sqrt{2}\ell. \tag{1.16}$$

If we increase ρ_∞ and N linearly with ℓ we should see consistent behavior in our discretization scheme. We found that adding 20ℓ to ρ_∞, and increasing N to preserve our value of $\Delta\rho$ is sufficient. We can compute the error in our numerical results by doubling N and looking at the difference between the two results.

Using our derived parameters and scaling, we found the first one hundred eigenvalues for $\ell = 0 \to 70$. We labeled the lowest eigenvalues $n = 1$ for each value of ℓ. Table 1.1 shows the first few eigenvalues for a range of ℓ. We can notice a few things immediately. Our data is within the upper bounds set in Asturias and Aragón [1] and as expected we do not find degenerate energies for different ℓs. We have found the spectrum of two dimensional hydrogen.

1.4 Curve Fitting

A reasonable idea is to take the basic structure of the spectrum that comes to us from the Bohr model and try to fit our data to it. Recall that the Bohr model Eqn (17) gives

$$\bar{E}_n = \frac{1 + \log 2}{2} + \log(n). \tag{1.17}$$

The Bohr model tacitly assumes zero orbital angular momentum and generally will not correctly predict the ground state. Indeed, this exact function does not quite work, even for $\ell = 0$. Instead we try a fit of the form

$$\bar{E}_n = A(\ell) + \log(n + C(\ell)) \tag{1.18}$$

for arbitrary ℓ. We have very little idea of the spectrum's dependence on ℓ, other than it should be nontrivial.[4]

For $\ell = 0 \to 70$ we found the best logarithmic fit using the lowest fifty eigenvalues.[5] Figure 1.1 illustrates that these fits correspond well to our data. We can also see a little divergence from our logarithmic fit in the large n and ℓ values. This corresponds

[3]The effective potential is the sum of the potential energy and the centrifugal potential, the term dependent on ℓ in the Hamiltonian.

[4]A perturbative approach to the Sommerfeld model predicts that $C(\ell)$ is linear and is done in Appendix A.

[5]We used a least squares fitting procedure in Mathematica, see Press et al. [13] for a good explanation and description of computing the error and parameters.

ℓ	0		1	
n	This work	Asturias and Aragón [1]	This work	Asturias and Aragón [1]
1	$0.52640 \pm 8 \times 10^{-5}$	$0.52664 \pm 3 \times 10^{-5}$	$1.38618 \pm 1.2 \times 10^{-6}$	$1.38621 \pm 2 \times 10^{-5}$
2	$1.66121 \pm 3 \times 10^{-5}$	$1.66134 \pm 2 \times 10^{-5}$	$2.00947 \pm 1.1 \times 10^{-6}$	$2.00951 \pm 2 \times 10^{-5}$
3	$2.17715 \pm 2 \times 10^{-5}$	$2.17724 \pm 1 \times 10^{-5}$	$2.39434 \pm 1.0 \times 10^{-6}$	$2.39437 \pm 1 \times 10^{-5}$
4	$2.51543 \pm 2 \times 10^{-5}$	$2.51553 \pm 1 \times 10^{-5}$	$2.67267 \pm 9.7 \times 10^{-7}$	$2.6727 \pm 1 \times 10^{-4}$
5	$2.76761 \pm 1 \times 10^{-5}$	$2.776 \pm 1 \times 10^{-3}$	$2.89061 \pm 9.4 \times 10^{-7}$	...
6	$2.96878 \pm 1 \times 10^{-5}$	...	$3.06966 \pm 9.2 \times 10^{-7}$	...

(a)

ℓ	2		3	
n	This work	Asturias and Aragón [1]	This work	Asturias and Aragón [1]
1	$1.84437 \pm 9.8 \times 10^{-8}$	$1.84440 \pm 4 \times 10^{-5}$	$2.15785 \pm 4.1 \times 10^{-8}$	$2.15785 \pm 1 \times 10^{-5}$
2	$2.27586 \pm 2.0 \times 10^{-7}$	$2.27654 \pm 3 \times 10^{-5}$	$2.48812 \pm 1.1 \times 10^{-7}$	$2.48812 \pm 1 \times 10^{-5}$
3	$2.58005 \pm 3.3 \times 10^{-7}$	$2.58021 \pm 2 \times 10^{-4}$	$2.73905 \pm 1.7 \times 10^{-7}$	...
4	$2.81447 \pm 3.8 \times 10^{-7}$	...	$2.94097 \pm 2.3 \times 10^{-7}$	...
5	$3.00496 \pm 3.8 \times 10^{-7}$	...	$3.20968 \pm 2.7 \times 10^{-7}$	...
6	$3.16531 \pm 4.2 \times 10^{-7}$	...	$3.25448 \pm 3.1 \times 10^{-7}$	...

(b)

Table 1.1: Table of our energy eigenvalues as compared to the upper bounds from Asturias and Aragón [1] for $n = 1 \to 6$ and $\ell = 0 \to 3$.

to a quadratic roll off,[6] the result of a less than ideal choice of ρ_∞ for our quantum numbers.

Looking at the parameters plotted in Figure 1.2, we can immediately see that our data has dependence on ℓ not predicted by the Bohr result. A seems to have some minimal dependence on ℓ, and C seems linear in ℓ. Note that the χ^2 values, which are a measure of "goodness of fit" with smaller values corresponding to better fits, are small. This agrees with our visual observation in Figure 1.1 that the fits are good. We see that the χ^2 peaks at around $\ell = 4$ but both the large ℓ states and the $\ell = 0$ state are well fit.

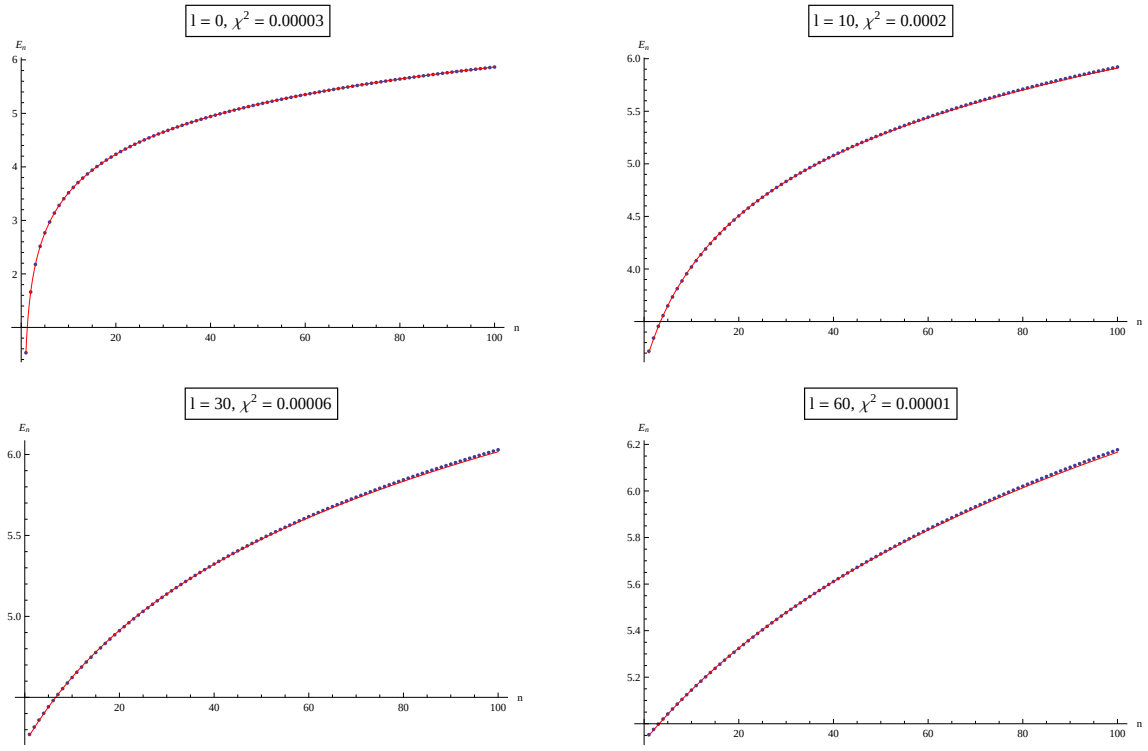

Figure 1.1: Plots of the first 100 eigenvalues with the best fits plotted on top for a range of ℓ.

We have made a compelling case that our fits are of the form $A(\ell)+\log(n+C(\ell))$, but we still have two unknown functions $A(\ell)$ and $C(\ell)$. Starting with $A(\ell)$ we have an idea that it could be constant plus some other behavior. The constant part is a result of the spectrum shifting as a function of r_0 which sets the zero of the potential. If we remove this offset, and multiply by -1, we find that the plot of the resulting values, the left hand side of Figure 1.3, looks suspiciously logarithmic. The best

[6] This is the result of picking up bound states of the infinite square well that our problem is in through our choice of boundary conditions.

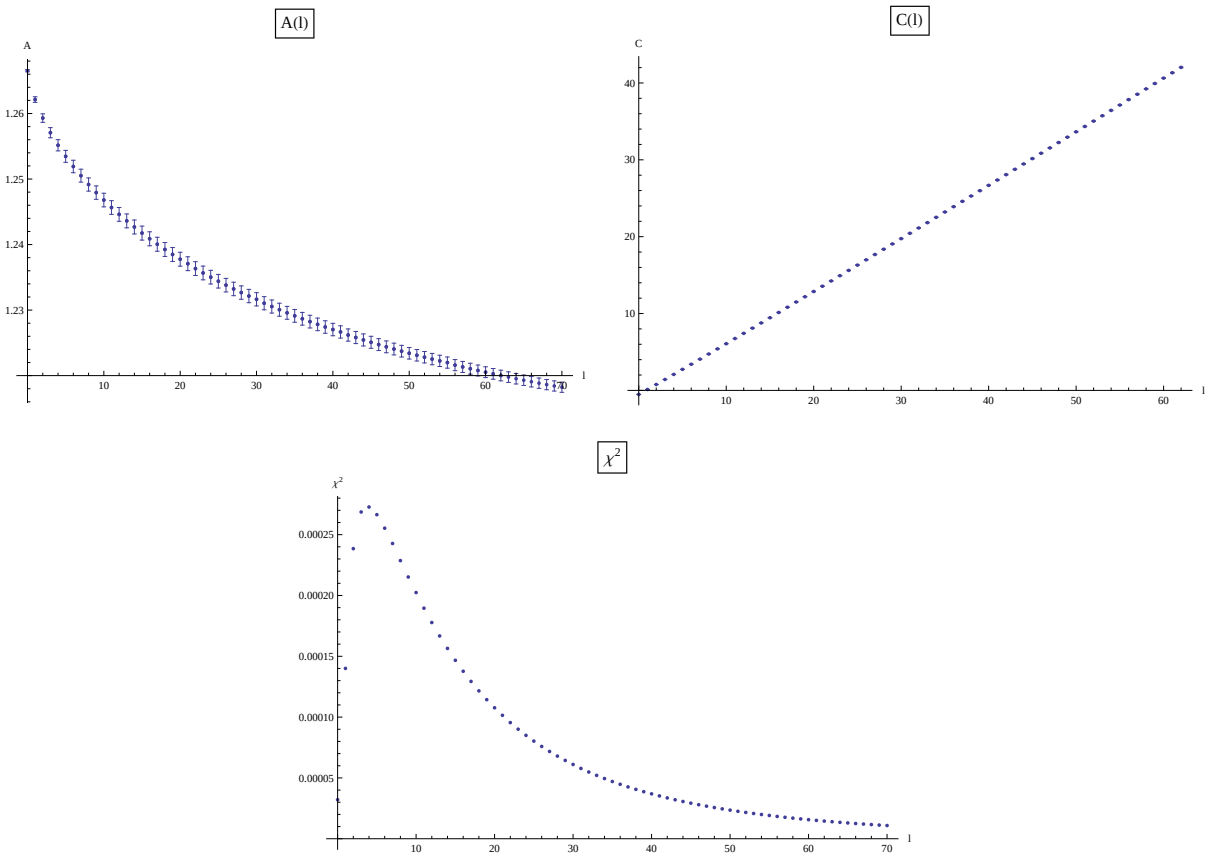

Figure 1.2: Plots of our fitting parameters as a function of ℓ with a constant B.

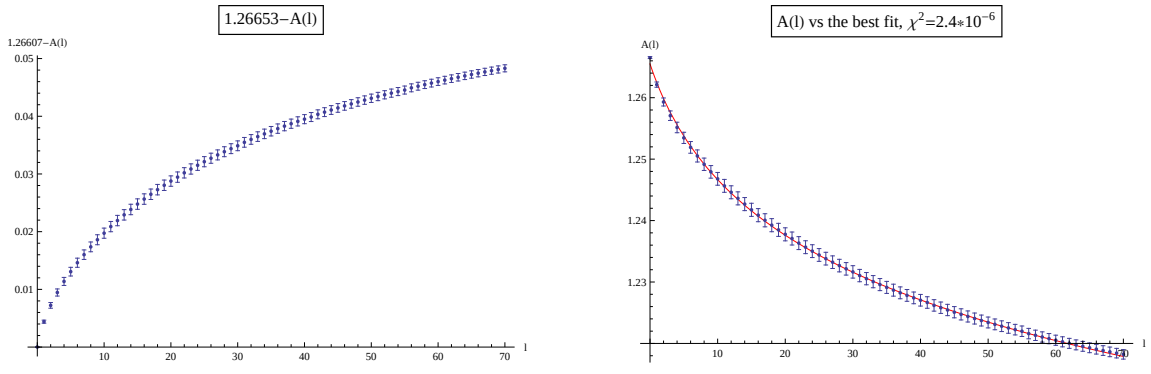

Figure 1.3: Plots of our scaled $A(\ell)$ on the left. On the right, is a plot of $A(\ell)$ versus the best fit.

logarithmic fit is

$$A(\ell) = (1.2959 \pm 3 \times 10^{-4}) - (0.0180 \pm 1 \times 10^{-4}) \log\left((5.4 \pm 0.11) + \ell\right) \tag{1.19}$$

with $\chi^2 = 2.4 \times 10^{-6}$. This best fit is shown on the right half of Figure 1.3. The small value of χ^2 leads us to conclude that this is an accurate fit for $A(\ell)$.

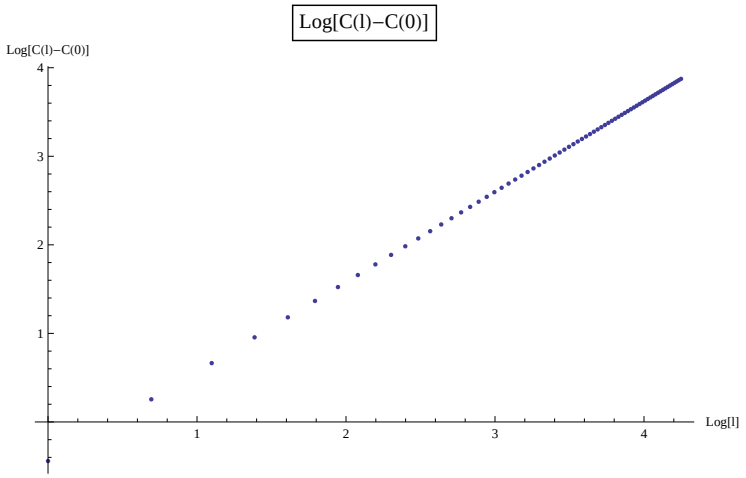

Figure 1.4: A log-log plot of our scaled $C(\ell)$. The data looks linear.

From the plot of our fitting parameters in Figure 1.2 we observe that $C(\ell)$ looks linear. An easy way to test for a linear relationship is to find the best linear fit on a log-log plot. We have two problems though: some of our values of C are negative and we have a point at 0. We can fix the negative values by subtracting from our data the point $C(0)$. Also we need to drop the point at $\ell = 0$. These two steps lead to the data shown in Figure 1.4. The best linear fit is

$$\log(C(\ell) - C(0)) = (-0.457 \pm 1.1 \times 10^{-3}) + (1.0191 \pm 3.4 \times 10^{-4}) \log \ell \tag{1.20}$$

and the resulting best fit for C(l) is

$$C(l) = -0.5217 + (0.633 \pm 1.1 \times 10^{-3}) \ell^{(1.0191 \pm 3.4 \times 10^{-4})} \tag{1.21}$$

with $\chi^2 = 0.0037$. This is a good value of χ^2 in relation to the scale of the values we are working with. It is nearly linear, just as the Sommerfeld model predicted.

With these two constants in place we can build up a fit for the energy eigenstates

$$\bar{E}_{n,\ell} = (1.2959 \pm 3 \times 10^{-4}) + \log\left(\frac{n - 0.5217 + (0.633 \pm 1.1 \times 10^{-3}) \ell^{(1.0191 \pm 3.4 \times 10^{-4})}}{\left((5.4 \pm 0.11) + \ell\right)^{(0.0180 \pm 1 \times 10^{-4})}}\right). \tag{1.22}$$

Figure 1.5 is a plot of the χ^2 value of the fits as a function of ℓ from $\ell = 0 \to 99$. From the figure we can see that the χ^2 values are small, indicative of the accuracy of

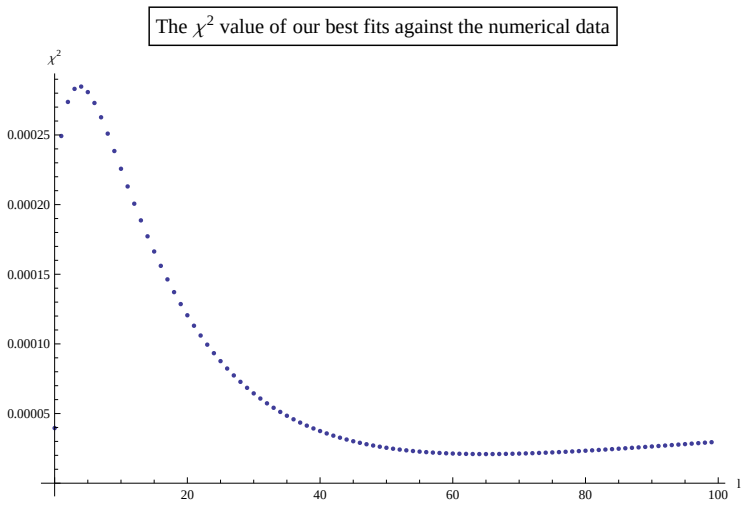

Figure 1.5: A plot of the χ^2 value for the first 100 eigenvalues of our best fit for the numerical data for $\ell = 0 \rightarrow 99$. We can see that our fits are relatively good because the χ^2 values are small.

our general fit. The Schrödinger solution corrects two of the deficiencies of the Bohr model: the ground state and angular momentum dependence. But it still does not include relativistic or dimension dependent effects. We could build up an extremely accurate periodic table using this model, as attempted by Asturias and Aragón [1], if we so desired.

There are some lingering problems though. The χ^2 has some ℓ dependence, which may be indicative of some fluctuations in the data for small nonzero ℓ. The numerical error is higher than we would like and we are only working with 71 values of ℓ and 50 values of n for each. With more computation time these two caveats are completely mendable.

Chapter 2

Higher Dimensional Solutions

Although the Coulomb potential and our logarithmic potential are most naturally defined in three and two dimensions respectively, they can be extended to an arbitrary numbers of dimensions. This is not just a toy problem, as we can find physical systems where these potentials are manifested in higher dimensional systems. For example, near a long straight wire in (3+1) dimensions we have a logarithmic potential. The Bohr model is insensitive to changing dimension, so for this particular question the Bohr model gives us no insight at all.

2.1 Coulomb in D dimensions

The radial portion of the Schrödinger equation in $(D+1)$ dimensions is [14]

$$-\frac{\hbar^2}{2m}\frac{1}{r^{D-1}}\frac{d}{dr}\left(r^{D-1}\frac{dR(r)}{dr}\right)+\left(\frac{\hbar^2}{2m}\frac{\ell(\ell+D-2)}{r^2}+V(r)\right)R(r)=ER(r). \quad (2.1)$$

Using the Coulomb potential our equation becomes

$$\frac{-\hbar^2}{2m}\left(R''(r)+\frac{D-1}{r}R'(r)\right)+\left(\frac{\hbar}{2m}\frac{\ell(\ell+D-2)}{r^2}-\frac{e^2}{4\pi\epsilon_0}\frac{1}{r}\right)R(r)=ER(r) \quad (2.2)$$

We can solve this equation for E using a series solution and find that this spectrum as a function of D and n is

$$E_{n,D}=\frac{-mc^2\alpha^2}{2\left(n+\frac{D-3}{2}\right)^2}. \quad (2.3)$$

This result recreates the known spectrum for (2+1) and (3+1) dimesnions [5, 4] and agrees with previously published results [14, 15].

We can make a few observations about Eq (2.3). First, in the large n limit, the spectrum is proportional to $\frac{1}{n^2}$, physically the effects of changing dimension are overwhelmed by increasing n. A second observation is that the $n=1, D=1$ state has an infinite negative energy.[1] A third observation is that the eigenvalues are

[1] Whether this is problematic is a subject of much debate, see Moss [15] for more information.

degenerate in ℓ because there is a large amount of symmetry in the D dimensional equation, which in three spatial dimensions is represented by the conservation of the Runge-Lenz vector.

2.2 The logarithmic potential in D dimensions

Now consider the logarithmic potential in higher dimensional spaces. The rationale for this is rather exploratory, rather than physically motivated. Beginning with the D dimensional Schrödinger equation and using the same nondimensionalization we introduced previously, we get

$$-\left(R''(\rho)+\frac{D-1}{\rho}R'(r)\right)+\left(\frac{\ell(\ell+D-2)}{\rho^2}+\log\rho\right)R(\rho)=\bar{E}R(\rho). \tag{2.4}$$

There is one issue that we must address before this is reduced to a numerical problem: we would like our operator to only have a second derivative so that our finite difference approximation is symmetric. To that end let $u(\rho)=\rho^{\frac{D-1}{2}}R(\rho)$ and our eigenvalue equation becomes [2]

$$-u''(\rho)+\left(\frac{\ell(\ell+D-2)+\frac{1}{4}(D-1)(D-3)}{\rho^2}+\log\rho\right)u(\rho)=\bar{E}u(\rho), \tag{2.5}$$

which reduces to what we expect when $D=2$. From here the numerical discretization is trivial.

2.2.1 Numerical Results

Before getting to the numerics, we should look at how the effective potential changes as a function of D to get an idea of how to scale ρ_∞. The minimum of this potential will give us some intuition,

$$V_{\text{eff}}=\frac{l(l+D-2)+\frac{1}{4}(D-1)(D-3)}{\rho^2}+\log\rho \tag{2.6}$$

which has a minimum at

$$\rho_{\min}=\sqrt{2\left(\ell(\ell+D-2)+\frac{1}{4}(D-1)(D-3)\right)}. \tag{2.7}$$

The minimum of the effective potential is roughly still linear plus a small bit in ℓ and has a small offset that will be proportional to D^2. For small D and ℓ the linear approximation we were using in the (2+1) case continues to hold. For large D and ℓ, we may have to be aware of this scaling.

[2] For $D\neq 2$ this substitution does not cause any problems with $\ell=0$. For $D=2$ and $\ell=0$ we use Eqn (1.14).

D	$A(\ell)$
2	$(1.2959 \pm 3 \times 10^{-4}) - (0.0180 \pm 1 \times 10^{-4}) \log((5.4 \pm 0.11) + \ell)$
3	$(1.2969 \pm 3 \times 10^{-4}) - (0.01824 \pm 8 \times 10^{-5}) \log((6.20 \pm 0.09) + \ell)$
4	$(1.2973 \pm 3 \times 10^{-4}) - (0.01834 \pm 8 \times 10^{-5}) \log((6.9 \pm 0.10) + \ell)$
5	$(1.2974 \pm 3 \times 10^{-4}) - (0.01835 \pm 9 \times 10^{-5}) \log((7.4 \pm 0.11) + \ell)$
6	$(1.2974 \pm 3 \times 10^{-4}) - (0.01835 \pm 9 \times 10^{-5}) \log((7.9 \pm 0.12) + \ell)$
7	$(1.2971 \pm 5 \times 10^{-4}) - (0.0183 \pm 1 \times 10^{-4}) \log((8.3 \pm 0.13) + \ell)$

Table 2.1: The fit for the parameter $A(\ell)$ as a function of D

Until we notice this effect we can run our code as if we were still in two dimensions using the same discretization parameters. We found the first hundred eigenvalues for the first seventy one states of orbital angular momentum, from $\ell = 0 \rightarrow 70$. Using the same procedure as used for the 2-dimensional parameters, we found the best fit of the form $A + \log(n + C)$ and then fit A and C as functions of ℓ, as shown in Table 2.1 and Table 2.2 respectively. We observe that the first term in $A(\ell)$ seems independent of D. This parameter should only be dependent on r_0, since it sets the zero of our potential and thus the zero of the energy spectrum. Similarly the multiplicative value in front of the logarithm seems constant as well, with a value around 0.018. Finally the parameter inside of the logarithm does increase with D as shown in Figure 2.1.

It is unclear whether we can discern the functional form of this behavior from our six data points. We have no intuition of what the fit is and the data have quite large error bars. Trying various fits with six data points results in nearly any function fitting nicely with a small χ^2 value, but we can not tell what is actually correct. With more data points we could find a form of this fit.

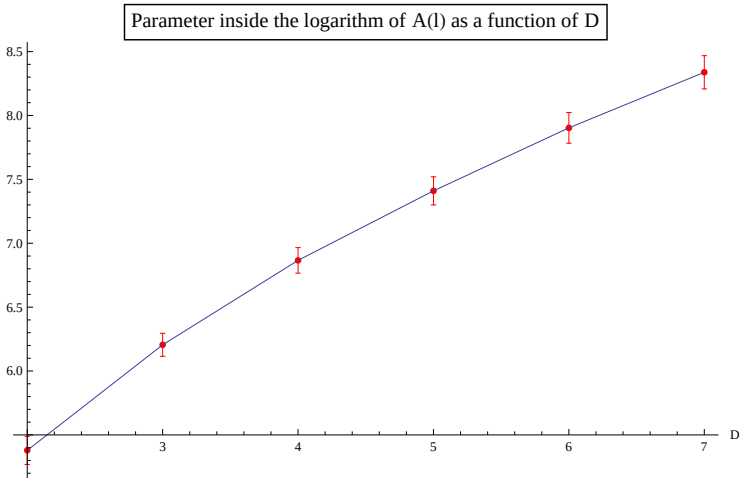

Figure 2.1: A plot of the constant inside the logarithm in $A(\ell, D)$ as a function of D.

For $C(\ell, D)$, the parameter in front of the ℓ dependent term seems to be roughly

D	$C(\ell)$
2	$-0.5217 + (0.633 \pm 1.1 \times 10^{-3})\ell^{(1.0191 \pm 3.4 \times 10^{-4})}$
3	$-0.2008 + (0.636 \pm 1.1 \times 10^{-3})\ell^{(1.0182 \pm 3.3 \times 10^{-4})}$
4	$0.1216 + (0.637 \pm 1.1 \times 10^{-3})\ell^{(1.0174 \pm 3.3 \times 10^{-4})}$
5	$0.4450 + (0.641 \pm 1.1 \times 10^{-3})\ell^{(1.0166 \pm 3.2 \times 10^{-4})}$
6	$0.7694 + (0.643 \pm 1.1 \times 10^{-3})\ell^{(1.0159 \pm 3.2 \times 10^{-4})}$
7	$1.0950 + (0.646 \pm 1.1 \times 10^{-3})\ell^{(1.0152 \pm 3.1 \times 10^{-4})}$

Table 2.2: The fit for the parameter $C(\ell)$ as a function of D

$-0.522 + 0.321(D-2)$ and the other two parameters seem constant.

From the parameters $A(\ell, D)$ and $C(\ell, D)$, we can build up a general fit,

$$E_{n,\ell,D} = 1.297 + \log\left(\frac{n - 0.522 + 0.321(D-2) + 0.64\ell^{1.02}}{(G(D)+\ell)^{0.0183}}\right) \tag{2.8}$$

where $G(D)$ is our yet unknown function. With more accurate data over a wider range of D this would not be difficult to nail down.

Like the Coulomb potential in D spatial dimensions, the dependence on dimension is small compared to the dependence on changing n and ℓ. We could confirm this by looking at the derivative of our energy with respect to n, ℓ, and D, but this is overkill. We can also generalize our results and conclude that for a hydrogenic system,the effect of dimension is only noticeable in low lying states and becomes negligible when the quantum numbers are large.

2.2.2 A semi-analytic result

Although we approached this result numerically, we can also approach it in a semi-analytic setting. We can rewrite Eqn 2.5 as

$$-u''(\rho) + \left(\frac{\ell^2 + (D-2)\ell + \frac{1}{4}(D-2)^2 - \frac{1}{4}}{\rho^2} + \log\rho\right)u(\rho) = \bar{E}u(\rho), \tag{2.9}$$

which we can further massage into

$$-u''(\rho) + \left(\frac{\left(\ell + \frac{1}{2}(D-2)\right)^2 - \frac{1}{4}}{\rho^2} + \log\rho\right)u(\rho) = \bar{E}u(\rho). \tag{2.10}$$

Defining $\tilde{\ell} = \ell + \frac{1}{2}(D-2)$, our equation becomes

$$-u''(\rho) + \left(\frac{\tilde{\ell}^2 - \frac{1}{4}}{\rho^2} + \log\rho\right)u(\rho) = \bar{E}u(\rho). \tag{2.11}$$

This equation is in the same form as Eqn (1.13), so the spectrum is the same as Eqn 1.22 with $\tilde{\ell}$ replacing ℓ:[3]

$$\bar{E}_{n,\tilde{\ell}} = 1.296 + \log\left(\frac{n - 0.522 + 0.633\tilde{\ell}^{1.019}}{\left(5.4 + \tilde{\ell}\right)^{0.018}}\right). \tag{2.12}$$

If we insert the definition of $\tilde{\ell}$ and Taylor expand to first order we find that the spectrum is

$$\bar{E}_{n,\ell,D} = 1.296 + \log\left(\frac{n - 0.522 + 0.323\ell^{0.019}(D-2) + 0.633\ell^{1.019}}{\left(5.4 + \frac{1}{2}(D-2) + \ell\right)^{0.018}}\right). \tag{2.13}$$

This new spectrum compares favorably to Eqn 2.8. As we saw in the numerical treatment, there is a term that is about $0.32(D-2)$ inside the logarithm, although now it is proportional to $\ell^{0.019}$ as well. We also now know that $G(D) = 5.4 + \frac{1}{2}(D-2)$, at least to first order in D.

We can apply this technique to other systems as well. For example, using the Coloumb potential we can find Eqn (2.3) from Eqn (6) using the same substitution.

[3]We are going to drop the error bars because we are working more qualitatively.

Chapter 3

Relativistic Solutions

Now that we know the spectrum if the electron moving at speeds much less than c, it is of interest to cover the other case: what happens when the electron is moving relativistically? The tools that we have developed thus far lose some of their potency. The Schödinger equation is not Lorentz invariant nor does it treat time and space equally. We could add higher order perturbative corrections derived from relativistic kinetic energy, but given the powerful numerical methods available to us it is more practical to instead use the Dirac equation.

3.1 The Two Dimensional Dirac Equation

In special relativity, we know that the quantity $E^2 - p^2c^2 = m^2c^4$ is invariant, meaning it is the same regardless of reference frame. If we let $\sqrt{p^2c^2 + m^2c^4}$ be the energy of a particle and $p \to -i\hbar\nabla$, we end up with relativistic quantum mechanics governed by the Klein-Gordon equation. Unfortunately the Klein-Gordon equation only describes the motion of bosons (particles with integer spin), and our system is two fermions (with half integer spin). So we need to think differently.

Dirac wanted a wave function that was first order in position and time. The general equation he wrote down was

$$E = c\sum_{i=1}^{2} \alpha_i p_i + \beta mc^2 \tag{3.1}$$

where α_i and β are matrices [9]. We can set the constants by looking at the square of the equation

$$E^2 = \beta^2 m^2 c^4 + mc^3 \sum_{i=1}^{2} \left(\alpha_i\beta + \beta\alpha_i\right) p_i + c^2 \sum_{i,j=1}^{2} \left(\alpha_i\alpha_j + \alpha_j\alpha_j\right) p_i p_j \tag{3.2}$$

and use

$$p^2c^2 + m^2c^4 = \beta^2 m^2 c^4 + mc^3 \sum_{i=1}^{2} \left(\alpha_i\beta + \beta\alpha_i\right) p_i + c^2 \sum_{i,j=1}^{2} \left(\alpha_i\alpha_j + \alpha_j\alpha_j\right) p_i p_j. \tag{3.3}$$

Exploiting the correspondence, we conclude that

$$\begin{aligned} \beta^2 &= \mathbb{I} \\ \alpha_i\beta + \beta\alpha_i &= 0 \\ \alpha_i\alpha_j + \alpha_j\alpha_j &= 2\delta_{ij}\mathbb{I} \end{aligned} \tag{3.4}$$

In addition, the matrices must be Hermitian so the Hamiltonian operator corresponds to an observable quantity. A set of matrices that fulfill these conditions are the Pauli matrices. The two dimensional Dirac Hamiltonian is then

$$H = -i\hbar c\left(\begin{pmatrix} 0 & 1 \\ 1 & 0 \end{pmatrix}\frac{\partial}{\partial x_1} + \begin{pmatrix} 0 & -i \\ i & 0 \end{pmatrix}\frac{\partial}{\partial x_2}\right) + \begin{pmatrix} 1 & 0 \\ 0 & -1 \end{pmatrix}mc^2 + V\mathbb{I}. \tag{3.5}$$

At this point we can multiply by ψ and find the spectrum.

In our systems the potential is radially symmetric, so we should naturally reparameterize into polar coordinates. We can let $x_1 = r\cos\theta$ and $x_2 = r\sin\theta$ and rewrite our Hamiltonian as

$$H = -i\hbar c\begin{pmatrix} 0 & e^{-i\theta} \\ e^{i\theta} & 0 \end{pmatrix}\frac{\partial}{\partial r} + \frac{\hbar c}{r}\begin{pmatrix} 0 & -e^{-i\theta} \\ e^{i\theta} & 0 \end{pmatrix}\frac{\partial}{\partial\theta} + \sigma_3 mc^2 + V\mathbb{I}. \tag{3.6}$$

Multiplying by $\psi(r,\theta)$, the wave equation is

$$\begin{aligned} E\psi(r,\theta) = &-i\hbar c\begin{pmatrix} 0 & e^{-i\theta} \\ e^{i\theta} & 0 \end{pmatrix}\frac{\partial\psi(r,\theta)}{\partial r} + \frac{\hbar c}{r}\begin{pmatrix} 0 & -e^{-i\theta} \\ e^{i\theta} & 0 \end{pmatrix}\frac{\partial\psi(r,\theta)}{\partial\theta} \\ &+ \sigma_3 mc^2\psi(r,\theta) + V\psi(r,\theta). \end{aligned} \tag{3.7}$$

We have successfully rewritten our equation in terms of the polar variables r and θ.

Using a separation of variables ansatz for our wave function, $\psi(r,\theta) = \begin{pmatrix} f(r)\Theta(\theta) \\ ig(r)\bar{\Theta}(\theta) \end{pmatrix}$, we get a set of coupled equations

$$\begin{aligned} \left(\frac{E - mc^2 - V}{\hbar c}\right)f &= \left(\frac{\bar{\Theta}}{\Theta}\frac{\partial}{\partial r} - \frac{i}{r}\frac{\bar{\Theta}'}{\Theta}\right)ge^{-i\theta} \\ \left(\frac{E + mc^2 - V}{\hbar c}\right)g &= -\left(\frac{\Theta}{\bar{\Theta}}\frac{\partial}{\partial r} + \frac{i}{r}\frac{\Theta'}{\bar{\Theta}}\right)fe^{i\theta}. \end{aligned} \tag{3.8}$$

Multiplying the previous two equations together gives

$$\left(\frac{E - mc^2 - V}{\hbar c}\right)\left(\frac{E + mc^2 - V}{\hbar c}\right)fg = -\left(\frac{\bar{\Theta}}{\Theta}\frac{\partial}{\partial r} - \frac{i}{r}\frac{\bar{\Theta}'}{\Theta}\right)g\left(\frac{\Theta}{\bar{\Theta}}\frac{\partial}{\partial r} + \frac{i}{r}\frac{\Theta'}{\bar{\Theta}}\right)f. \tag{3.9}$$

Expanding the right hand side, we find that every term has θ dependence of form $\frac{\bar{\Theta}'}{\Theta}\frac{\Theta'}{\Theta}$, $\frac{\Theta'}{\Theta}$, $\frac{\bar{\Theta}'}{\bar{\Theta}}$, or no θ dependence at all. We conclude that the values $\frac{\Theta'}{\Theta}$ and $\frac{\bar{\Theta}'}{\bar{\Theta}}$ must

be constants, im and in respectively. We can write these solutions as $\Theta(\theta) = \frac{1}{\sqrt{2\pi}} e^{im\theta}$ and $\bar{\Theta}(\theta) = \frac{1}{\sqrt{2\pi}} e^{in\theta}$. Plugging these new definitions in we obtain

$$\begin{aligned} \left(\frac{E - mc^2 - V}{\hbar c}\right) f e^{im\theta} &= \frac{\partial g}{\partial r} e^{i(n-1)\theta} + \frac{n}{r} g e^{(n-1)i\theta} \\ \left(\frac{E + mc^2 - V}{\hbar c}\right) g e^{in\theta} &= -\frac{\partial f}{\partial r} e^{i(m+1)\theta} + \frac{m}{r} f e^{i(m+1)\theta}. \end{aligned} \tag{3.10}$$

We would like these phases to cancel so we require

$$m = n - 1$$

and can relate m and n by a factor κ, with

$$m = \kappa - 1/2, \quad n = \kappa + 1/2. \tag{3.11}$$

We think of κ as the total angular momentum, the sum of the orbital angular momentum ℓ along with the contribution from the electron's spin $\pm 1/2$. It is a half integer because $\ell \pm 1/2 = 1/2, 3/2, \ldots$ With these two steps our initial ansatz has now become $\psi(r,\theta) = \frac{1}{(2\pi)^{1/2}} \begin{pmatrix} f(r) e^{i(\kappa - 1/2)\theta} \\ i g(r) e^{i(\kappa + 1/2)\theta} \end{pmatrix}$ and the differential equation simplifies to

$$\begin{aligned} \left(\frac{E - mc^2 - V}{\hbar c}\right) f &= \left(\frac{\partial g}{\partial r} + \frac{\kappa + 1/2}{r} g\right) \\ \left(\frac{E + mc^2 - V}{\hbar c}\right) g &= -\left(\frac{\partial f}{\partial r} - \frac{\kappa - 1/2}{r} f\right). \end{aligned} \tag{3.12}$$

We can solve for the relativistic Coulomb spectrum using a series solution, and find that the spectrum is

$$E_{n,\kappa} = \pm mc^2 \left[1 + \frac{\alpha^2}{\left(n - |\kappa| - 1/2 + \sqrt{\kappa^2 - \alpha^2}\right)^2}\right]^{-1/2}. \tag{3.13}$$

When we Taylor expand to second order in α we recover the rest energy and the Schrödinger spectrum Eqn (6)

$$E_{n,\kappa} \approx \pm \left(mc^2 - \frac{mc^2 \alpha^2}{2\left(n - 1/2\right)^2} + O(\alpha^3)\right). \tag{3.14}$$

The spectrum in Eqn (3.13) is symmetric: for every positive energy bound state there is a corresponding negative energy state representing an antiparticle. We should expect to get back a similar symmetry with our logarithmic potential. We will choose to ignore the negative energy states and focus on the positive energy states, but the behavior will be the same for the negative energy states with an overall sign change.

Returning to the logarithmic potential, our coupled differential equations are

$$\begin{aligned}\left(\frac{E}{\hbar c}-\frac{mc}{\hbar}-\frac{\Omega}{\hbar c}\log(r/r_0)\right)f&=\left(\frac{\partial}{\partial r}+\frac{\kappa+1/2}{r}\right)g\\ \left(\frac{E}{\hbar c}+\frac{mc}{\hbar}-\frac{\Omega}{\hbar c}\log(r/r_0)\right)g&=-\left(\frac{\partial}{\partial r}-\frac{\kappa-1/2}{r}\right)f.\end{aligned}\tag{3.15}$$

Given that we are unable to analytically solve this system, we will again use numerical methods. We should nondimensionalize using the same scaling of the energy that we used for the non-relativistic system, so we can compare our numerical results. To that end let $r=\rho_0\rho$ and $r_0=\rho_0$, where $\rho_0=\sqrt{\frac{\hbar^2}{2m\Omega}}$. Similarly, we want our energy scale to be the same as in the Schrödinger case. Letting $E=\Omega\bar{E}$ and $\nu=mc^2/\Omega$, we find a set of equations,

$$\begin{aligned}\bar{E}f&=(\nu+\log(\rho))\,f+\sqrt{2\nu}\left(\frac{\partial}{\partial\rho}+\frac{\kappa+1/2}{\rho}\right)g\\ \bar{E}g&=(-\nu+\log(\rho))\,g-\sqrt{2\nu}\left(\frac{\partial}{\partial\rho}-\frac{\kappa-1/2}{\rho}\right)f.\end{aligned}\tag{3.16}$$

We can think of ν as a measure of how relativistic our system is. In the limit where ν is large we should recover the non-relativistic spectrum plus the rest energy; in the limit where ν is small relativistic effects should be more pronounced.

3.2 The non-relativistic and highly relativistic limits

Equations (3.16) govern the behavior of our system. We noticed earlier that when ν is large, we should get back the Schrödinger spectrum plus the rest energy. We should see if we can get this limit analytically as well as qualitatively. Working from Eqn (3.16) with $\kappa=1/2$ and defining $\bar{E}_s=\bar{E}-\nu$, where $\bar{E}_s$ should be the Schrödinger energies for large ν, our equations become

$$\begin{aligned}\left(\bar{E}_s-\log\rho\right)f&=\sqrt{2\nu}g'+\sqrt{2\nu}\frac{g}{\rho}\\ \left(\bar{E}_s+2\nu-\log\rho\right)g&=-\sqrt{2\nu}f'.\end{aligned}\tag{3.17}$$

Combining them into one second order system gives

$$\begin{aligned}\left(\bar{E}_s-\log\rho\right)\left(\bar{E}_s+2\nu-\log\rho\right)^2f=&-2\nu\left(\bar{E}_s+2\nu-\log\rho\right)f''\\ &-2\nu\left(\bar{E}_s+2\nu-\log\rho+1\right)\frac{f'}{\rho}.\end{aligned}\tag{3.18}$$

This equation is exact. In the limit where $\nu\gg1$, we expect $\nu\gg\bar{E}_s$, allowing us to simplify our equation a bit

$$\left(2\nu\bar{E}_s-2\nu\log\rho+(\log\rho)^2\right)f=-2\nu f''-2\nu\frac{f'}{\rho}.\tag{3.19}$$

We can show that $f \to 0$ faster than $(\log\rho)^2 f \to \infty$. This leaves

$$\bar{E}_s f = -f'' - \frac{f'}{\rho} + (\log\rho) f, \tag{3.20}$$

which is exactly the radial time independent Schrödinger equation with $\ell = 0$, Eqn (1.9). We therefore see that our function has the appropriate large ν limit, which is reassuring.

We should also look at the highly relativistic regime where $\nu \ll 1$. Letting $\bar{f} = \sqrt{\rho} f$ and $\bar{g} = \sqrt{\rho} g$, as we did in the Schrödinger case, our system becomes

$$\begin{aligned} \bar{E}\bar{f} &= (\nu + \log(\rho))\,\bar{f} + \sqrt{2\nu}\left(\frac{\partial}{\partial\rho} + \frac{\kappa}{\rho}\right)\bar{g} \\ \bar{E}\bar{g} &= (-\nu + \log(\rho))\,\bar{g} - \sqrt{2\nu}\left(\frac{\partial}{\partial\rho} - \frac{\kappa}{\rho}\right)\bar{f}. \end{aligned} \tag{3.21}$$

We can combine our coupled first order equations into one second order equation and replace terms like $\bar{E} - \nu$ with $\bar{E}$ because we expect $\bar{E} \gg \nu$, giving

$$\begin{aligned} \left(2\kappa\nu + \bar{E}\left(-2\kappa(1+\kappa)\nu + \rho^2\bar{E}^2\right) + \log\rho\left(2\kappa(1+\kappa)\nu - 3\rho^2\bar{E}^2 + \rho^2(3\bar{E} - \log\rho)\log\rho\right)\right) g \\ +2\rho\nu\left(g' - \rho(-\bar{E} + \log\rho)g''\right) = 0. \end{aligned} \tag{3.22}$$

Since ν is small we can ignore terms that are constants multiplied by ν, yielding

$$g\left(\bar{E}\left(\rho^2\bar{E}^2\right) + \log\rho\left(-3\rho^2\bar{E}^2 + \rho^2(3\bar{E} - \log\rho)\log\rho\right)\right) + 2\rho\nu\left(g' - \rho(-\bar{E} + \log\rho)g''\right) = 0. \tag{3.23}$$

The term proportional to g factors, finally giving

$$\left(\bar{E} - \log\rho\right)^3 g + \frac{2\nu}{\rho}g' + 2\nu(\bar{E} - \log\rho)g'' = 0. \tag{3.24}$$

This equation does not immediately seem analytically tractable. It does tell us that in the small ν limit we should not expect any effects from our choice of κ. What is more interesting is that we appear to no longer have an eigenvalue problem – this may create problems with our numerical methods in this limit.

3.3 Numerics

Now that we have a very good idea of what to expect, we can employ our numerical method to discover the various fine points of this model. Applying our finite difference scheme to Eqn (3.21) gives

$$\begin{aligned} \bar{E}\bar{f}_j &= (\nu + \log(j\Delta\rho))\,\bar{f}_j + \sqrt{2\nu}\left(\frac{\bar{g}_{j+1} - \bar{g}_{j-1}}{2\Delta\rho} + \frac{\kappa\bar{g}_j}{j\Delta\rho}\right) \\ \bar{E}\bar{g}_j &= (-\nu + \log(j\Delta\rho))\,\bar{g}_j + \sqrt{2\nu}\left(\frac{\bar{f}_{j-1} - \bar{f}_{j+1}}{2\Delta\rho} + \frac{\kappa\bar{f}_j}{j\Delta\rho}\right). \end{aligned} \tag{3.25}$$

We observe that we can embed values of $\bar{g}$ and $\bar{f}$ into a vector and from this build a symmetric matrix representation of our operator.[1] We should be aware that our numerical calculations will be twice as big, since our discrete matrix will be $2N \times 2N$. This is necessary to capture the behavior of our coupled system. The more exciting numerical point is that because of the way everything is scaled our results will be immediately comparable to those from the Schrödinger spectrum and we can use the same discretization parameters we used for Schrödinger, as well.

We should also be cognizant of what sort of internal scaling we can do to make our numerics more efficient. We know from the Bohr model, in the large ν and small ν limits, that the eigenvalues we want should be roughly offset from zero by ν and $\frac{1+\log \nu}{2}$ respectively. These are limits of our function $P(\nu)$ from Eqn (24). If we subtract $P(\nu)$ from our data we should, according to the relativistic Bohr model, expect to recover the Schrödinger spectrum, or something similar to it, for all ν.

3.4 $\nu \gg 1$

The simpler regime to think about is the large ν regime. We expect our eigenvalues to be roughly $\bar{E}_s + \nu$, so we can subtract off $P(\nu)$ and expect our eigenvalues to be small and positive.

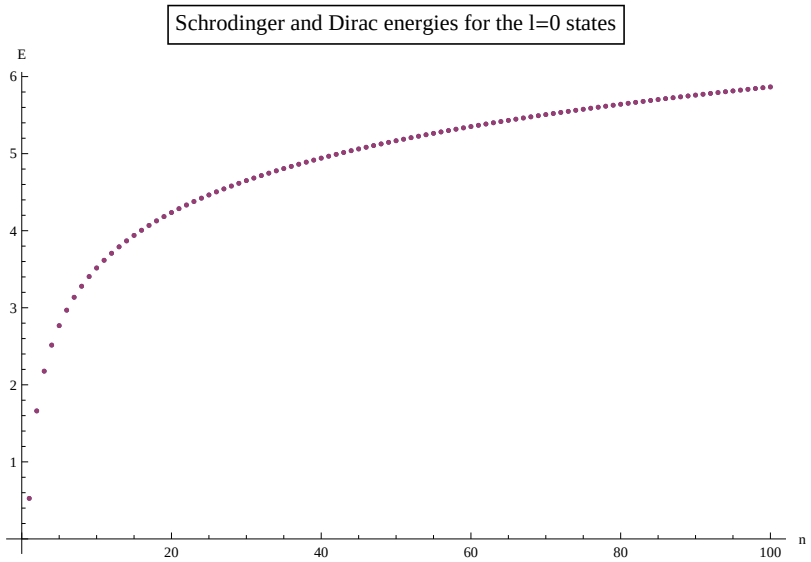

Figure 3.1: A plot of the spectrum from the Schrödinger and Dirac equations for $l = 0$ with ν substracted. For the Dirac results, we took every other point starting with the first because we get a mixing of eigenvalues of both the $\ell = 0$ and $\ell = 1$ states. The two sets of values are visually indistinguishable.

[1] This embedding is further explained in Franklin and Garon [3].

	Dirac	Schrödinger	
n	$\kappa = \frac{1}{2}$	$\ell = 0$	$\ell = 1$
1	$0.5263 \pm 2 \times 10^{-4}$	$0.526395 \pm 8 \times 10^{-5}$	
2	$1.38613 \pm 4 \times 10^{-5}$		$1.38618 \pm 1 \times 10^{-6}$
3	$1.66115 \pm 7 \times 10^{-5}$	$1.66121 \pm 3 \times 10^{-5}$	
4	$2.00943 \pm 3 \times 10^{-5}$		$2.00947 \pm 1 \times 10^{-6}$
5	$2.17711 \pm 5 \times 10^{-5}$	$2.17715 \pm 2 \times 10^{-5}$	
6	$2.39430 \pm 3 \times 10^{-5}$		$2.39434 \pm 1 \times 10^{-6}$
7	$2.51539 \pm 4 \times 10^{-5}$	$2.51543 \pm 2 \times 10^{-5}$	
8	$2.67263 \pm 3 \times 10^{-5}$		$2.67267 \pm 1 \times 10^{-6}$
9	$2.76758 \pm 4 \times 10^{-5}$	$2.76761 \pm 1 \times 10^{-5}$	
10	$2.89057 \pm 3 \times 10^{-5}$		$2.89061 \pm 1 \times 10^{-6}$

Table 3.1: A table of our energy eigenvalues from the Dirac equation in the highly non-relativistic regime, $\nu = 10^8$, as compared to the energy eigenvalues from the Schrödinger equation from Table 1.1 for $n = 1 \to 10$ and $\kappa = 1/2$.

For $\rho_\infty = 400$, $N = 50000$, $\kappa = 1/2 \to 15/2$ in steps of 1, and $\nu = 10^8$, we found the first three hundred hundred eigenvalues. Table 3.1 displays specifically the $\kappa = 1/2$ case.[2] Referring back to Table 1.1, we see that some of these eigenvalues are $\ell = 0$ states and some are $\ell = 1$ states of the Schrödinger spectrum. We also notice that the spectra are visually indistinguishable, see Figure 3.1. This is because for a given κ we have two possible values of ℓ. κ is the total angular momentum $\ell \pm 1/2$, and so we can get $\kappa = 3/2$, for example, from either $\ell = 1$ or $\ell = 2$. Since the nonrelativistic spectrum of our potential is not degenerate in ℓ we should expect to get a mixing of two ℓ states for a given κ. If we had degeneracy in ℓ, as with Coulomb potential, we would not notice this effect.

We can extract just the $\ell = 1$ states of the Dirac spectrum by taking every other point, and find the best fit of the Schrödinger form, which gives us $\bar{E}_{n,1} = 1.26212 + \log(n+0.1213)$. Earlier we found that this best fit should be $1.26213+\log(n+0.1214)$. The difference in the parameters between these two fits is within the margin of error of each of the fitting parameters. We get similar results for other states of orbital angular momentum as well, showing that this limit does indeed agree with the non-relativistic results.

3.5 $\nu \approx 1$

As we shrink ν down from its initially lofty values to something around $\nu \approx 1$ we should begin to see relativistic effects.

Using $N = 5000$, $\rho_\infty = 50$, $\kappa = 1/2$ & $3/2$, we found the first few energy eigenstates as $\nu = 1 \to 6$ in steps of 0.1, (figures 3.2 and 3.3). The error in this data is all

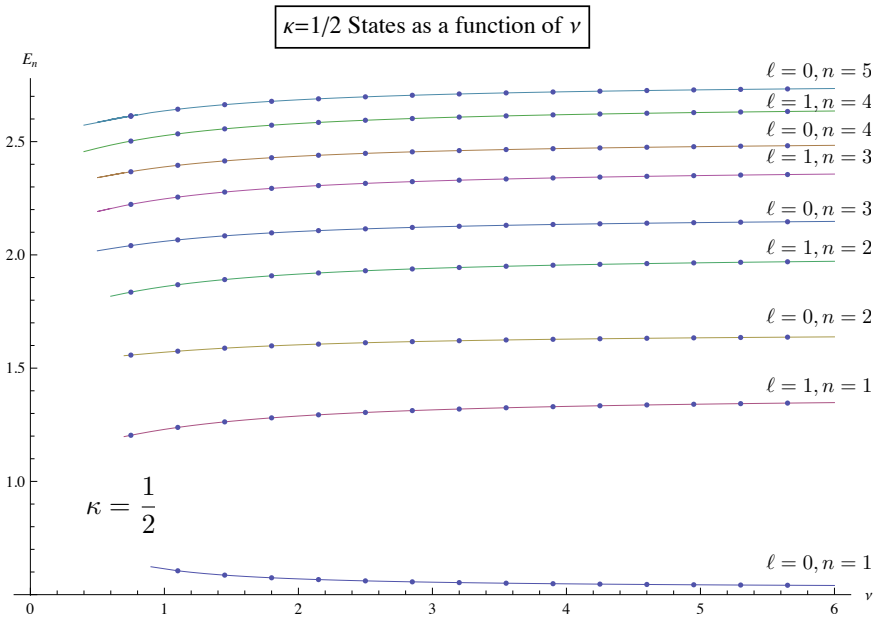

Figure 3.2: The spectrum for $\kappa = 1/2$ as a function of ν with $P(\nu)$ subtracted.

relatively large, on the order of 10^{-3}.[3]

We observe that as we decrease ν the ground state energy increases and the excited state energies decrease. What is most exciting about this is that the relativistic spectrum is the Schrödigner spectrum plus $P(\nu)$ plus what seem to be additional relativistic effects. These extra corrections are small. Looking at the two plots we notice that the spectra have significant κ dependence, unlike what we predict in the small ν limit Eqn (3.24). If we look at just the ground state and first excited state for $\ell = 1$, Figures 3.4 and 3.5, we see a nontrivial κ dependence.

This lovely story is shattered by an inability to probe downward into $\nu \ll 1$. This seems inexplicable because we have an eigenvalue problem, at least in a coupled form, and a robust method. It may be that our eigenvalue routine is unstable for our matrix discretization in the small ν regime but it could also be, as our analytic work in Eqn (3.24) suggested, that something odd happens when $\nu \approx 1$.

[2]We only show data from $\kappa = 1/2$ because the results are similar for all other values of κ.

[3]If we decrease the numerical error by increasing N, the qualitative behavior is unchanged. We choose $N = 5000$ because we could find the eigenvalues quickly.

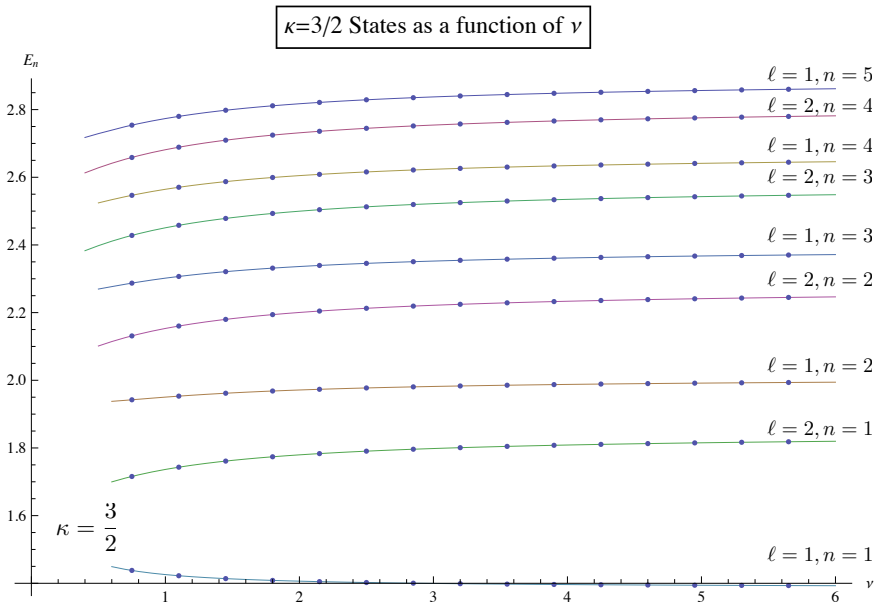

Figure 3.3: The spectrum for $\kappa = 3/2$ as a function of ν with $P(\nu)$ subtracted.

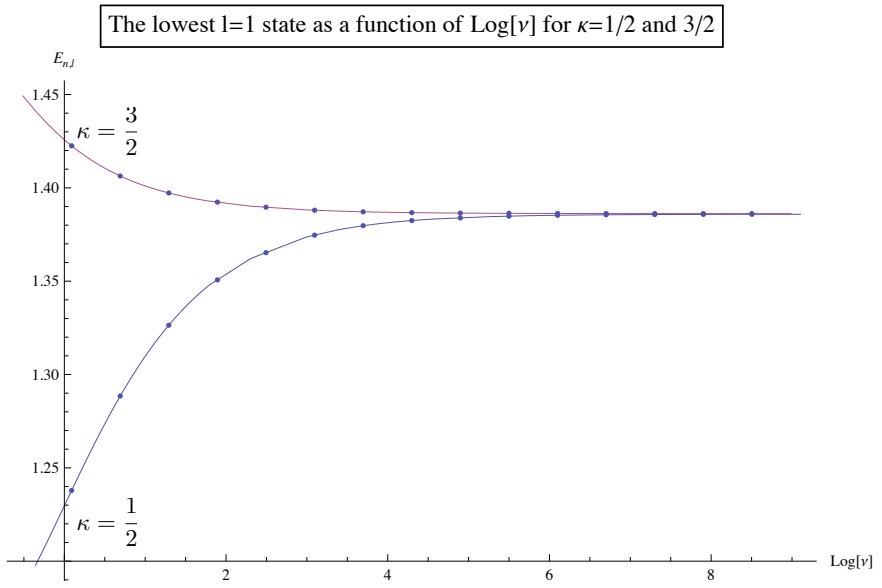

Figure 3.4: The lowest $\ell = 1$ state as a function of $\log \nu$ for $\kappa = 1/2$ and $\kappa = 3/2$.

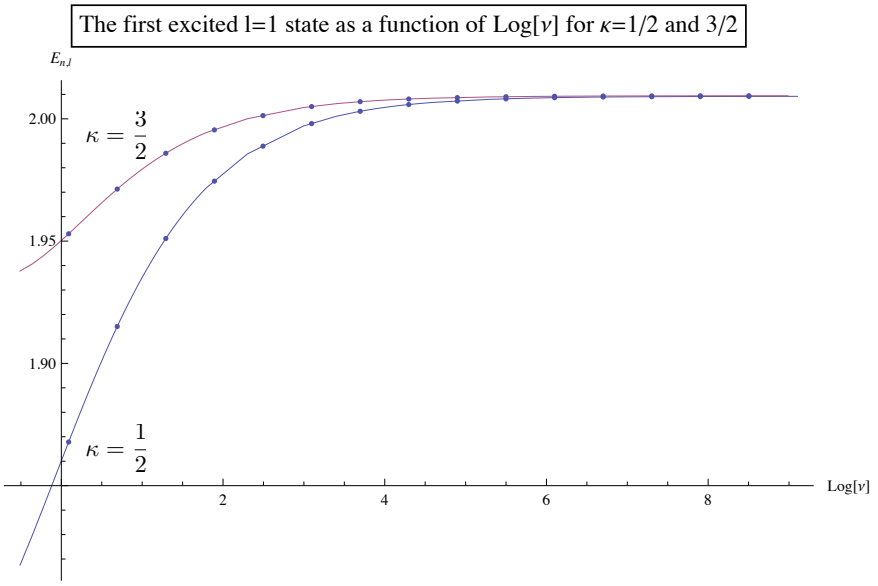

Figure 3.5: The first excited for $\ell = 1$ state as a function of $\log \nu$ for $\kappa = 1/2$ and $\kappa = 3/2$.

Conclusion

Our investigation into the spectrum of hydrogen with a logarithmic central potential comes to an end having made quite a bit of progress. We discovered an extremely robust general form of the spectrum of the two dimensional hydrogen atom. We investigated the spectrum of hydrogen with our logarithmic potential in an arbitrary number of dimensions and found solid quantitative predictions of the spectrum. Finally, we explored the behavior of two dimensional relativistic hydrogen and found that it shares some similarities with the Schrödinger spectrum.

These three results have been supported and motived by what we see as the moral of this thesis, that the Bohr model is an extremely strong tool in the study of quantum mechanical systems. It correctly predicted many of the qualitative features of both the Schrödinger and Dirac spectra, as well as the relationship between them. This was unexpected and rather pleasantly surprising. The corrections that we did find were beyond the scale of the model.

Further explorations of relativistic and higher dimensional spectra are possible and should be pursued. There are various ways of interpolating between logarithmic and $1/r$ potentials, and between two and three dimensions, that would hopefully shine some light on the relatively complex behavior of the spectrum. One could also start looking at modifications to electromagnetism such as Born-Infeld or Chern-Simons theory or look at perturbative solutions to problems in two dimensions. The extensions are numerous, but we would like to warn whoever may follow in this effort that numerical error and minus signs are one's enemy and utmost care must be taken to minimize their effect.

Appendix A

The Sommerfeld model

The perturbative Sommerfeld model provides a qualitative prediction of the behavior of $C(\ell)$ in the Schrödinger spectrum.

A.1 Perturbative Sommerfeld

The Sommerfeld model is a generalization of the Bohr model to open and generally noncircular orbits. It uses two quantization conditions

$$\oint p_\theta d\theta = hn_\theta \tag{A.1}$$

and

$$\oint p_r dr = hn_r \tag{A.2}$$

where p_r and p_θ are the momenta in the $\hat{r}$ and $\hat{\theta}$ directions. The quantization condition on p_θ returns the familiar condition, $L = \hbar n_\theta$, which is the Bohr quantization condition if $n = n_\theta$. For the systems we would like to look at we will not be able to necessarily solve the the quantization condition for n_r analytically so we take a perturbative approach, using nearly circular orbits.

To begin, for an orbit at radius r we know that the energy is

$$E = \frac{1}{2}m\dot{r}^2 + \frac{L^2}{2mr^2} + V(r) \tag{A.3}$$

with a corresponding equation of motion

$$m\ddot{r} = \frac{L^2}{mr^3} - V'(r). \tag{A.4}$$

For a circular orbit of radius $\tilde{r}$, these equations reduce to

$$\tilde{E} = \frac{L^2}{2m\tilde{r}^2} + V(\tilde{r}) \tag{A.5}$$

and

$$0 = \frac{L^2}{m\tilde{r}^3} - V'(\tilde{r}). \tag{A.6}$$

We can write the angular velocity $\tilde{\Omega}$ of this system as $L/m\tilde{r}^2$, by the conservation of angular momentum. We want to look at a small perturbation off the circular orbit so we let $r = \tilde{r} + \eta(t)$, and the equation of motion becomes

$$\ddot{\eta} = \frac{L^2}{m^2\tilde{r}^3}\left(1 - 3\frac{\eta}{\tilde{r}}\right) - \frac{1}{m}\left(V'(\tilde{r}) + \eta V''(\tilde{r})\right). \tag{A.7}$$

The quantity $\frac{L^2}{\bar{r}^3} - \frac{1}{m}V'(\bar{r}) = 0$ by Eqn (A.6), and defining $\omega^2 = 3\frac{L^2}{m^2\tilde{r}^4} + \frac{1}{m}V''(\tilde{r})$ our equation simplifies to

$$\ddot{\eta} = -\omega^2\eta \tag{A.8}$$

with solution

$$\eta = s_0\cos(\omega t) \tag{A.9}$$

where s_0 is a constant. Using this perturbation in Eqn (A.3), we find that the energies are

$$E = \frac{1}{2}m\dot{\eta}^2 + \frac{L^2}{2m\tilde{r}^2}\left(1 + \frac{\eta}{\tilde{r}}\right)^{-2} + V(\tilde{r} + \eta). \tag{A.10}$$

Taylor expanding we find this simplifies to

$$E = \tilde{E} + \frac{1}{2}m\omega^2 s_0^2. \tag{A.11}$$

That is, the energy is a sum of the unperturbed energy plus a contribution from the oscillating radial behavior. Now that we have an expression for E, we apply the Sommerfeld quantization condition Eqn (A.2), and evaluate over one revolution. We find that the integral evaluates to

$$hn_r = \frac{1}{2}ms_0^2\tilde{\Omega}^2\left(\frac{2\pi}{\tilde{\Omega}} - \frac{1}{2\omega}\sin\left(4\pi\frac{\omega}{\tilde{\Omega}}\right)\right). \tag{A.12}$$

Solving for $\frac{1}{2}ms_0^2\omega^2$, we find that the energy of our perturbed orbits is

$$E = \bar{E} + \hbar n_r\tilde{\Omega}\left(1 - \frac{\tilde{\Omega}}{4\pi\omega}\sin\left(4\pi\frac{\omega}{\tilde{\Omega}}\right)\right)^{-1}. \tag{A.13}$$

Using $\tilde{\Omega} = L/m\tilde{r}^2$ and the quantization condition $L = \hbar n_\theta$, gives:

$$E = \bar{E} + \hbar n_r\tilde{\Omega}\left(1 - \frac{\hbar n_\theta}{4\pi\omega m\tilde{r}^2}\sin\left(\frac{4\pi\omega m\tilde{r}^2}{\hbar n_\theta}\right)\right)^{-1}. \tag{A.14}$$

A.2 Sommerfeld with the logarithmic potential

We can find the Sommerfeld spectrum of the logarithmic potential. Looking at Eqn (A.6) we can find

$$\tilde{r} = L\sqrt{\frac{1}{m\Omega}} \tag{A.15}$$

where $L = n_\theta \hbar$. Inserting this result and our definition of r_0, and solving for $\tilde{E}$, we get

$$\tilde{E} = \Omega\left(\frac{1+\log 2}{2} + \log n_\theta\right) \tag{A.16}$$

which is exactly the energy spectrum from the Bohr model. Using this result to look at the perturbed energies, we get

$$E = \Omega\left(\frac{1+\log 2}{2} + \log n_\theta\right) + \hbar n_r \tilde{\Omega}\left(1 - \frac{\tilde{\Omega}}{4\pi\omega}\sin\left(4\pi\frac{\omega}{\tilde{\Omega}}\right)\right)^{-1}. \tag{A.17}$$

We can find that $\tilde{\Omega} = \frac{\Omega}{L}$ and $\omega = \sqrt{2}\frac{\Omega}{L}$, which makes our energies

$$\bar{E} = \frac{1+\log 2}{2} + \log n_\theta + \frac{n_r}{n_\theta}\left(1 - \frac{1}{4\sqrt{2}\pi}\sin\left(4\sqrt{2}\pi\right)\right)^{-1}. \tag{A.18}$$

where $\bar{E} = E/\Omega$. Also let $\sigma = \left(1 - \frac{1}{4\sqrt{2}\pi}\sin\left(4\sqrt{2}\pi\right)\right)^{-1} = 0.953$, and our energies become

$$\bar{E} = \frac{1+\log 2}{2} + \log n_\theta + \sigma\frac{n_r}{n_\theta}. \tag{A.19}$$

Since we are working in the limit where our orbits are nearly circular, we can assume that $n_r \ll n_\theta$. In this limit

$$\sigma\frac{n_r}{n_\theta} \approx \log\left(1 + \sigma\frac{n_r}{n_\theta}\right) \tag{A.20}$$

which makes our energies

$$\bar{E} = \frac{1+\log 2}{2} + \log\left(n_\theta + \sigma n_r\right). \tag{A.21}$$

Our usual quantum numbers n and ℓ will be some combination of n_θ and n_r, independent of how these quantum numbers combine, the argument inside the logarithm will be $n + C(\ell)$ where C is linear in ℓ.

Appendix B

Code Snippits

The following code is used to generate the matrix discretization of the (D+1) dimensional Schrödinger equation with a logarithmic potential, Eqn (2.5):

```
SymmetricSchLog[pinf_,NN_, L_,D_] :=
        Module[{Mat,ret,d,l,sdata,dp,idex,p},
        dp = pinf/NN;
        l=L(L+D-2);
        d=-.75+D-.25D^2;
        sdata={};

        For[idex=2,idex<=NN-1,idex=idex+1,
                p = idex dp;
                sdata=Join[sdata,{{idex,idex}-> (Log[p] +(l-d)/p^2+ 2.0/dp^2),
                        {idex,idex+1}-> -1.0/dp^2 ,{idex,idex-1} -> -1.0/dp^2}];
        ];

        idex=1;
        p = idex dp;
        sdata=Join[sdata,{{idex,idex}-> (Log[p] +(l-d)/p^2+ 2.0/dp^2),
                {idex,idex+1}-> -1.0/dp^2}];

        idex=NN;
        p = idex dp;
        sdata=Join[sdata,{{idex,idex}-> (Log[p] +(l-d)/p^2+ 2.0/dp^2),
                {idex,idex-1}->- 1.0/dp^2}];

        Mat =SparseArray[sdata];
        Return[Mat];
        ]
```

The following code is used to generate the matrix discretization of the (2+1) dimensional Dirac equation with a logarithmic potential, Eqn (3.16):

```
P[v_]:=v Sqrt[2/(-1+Sqrt[4v^2+1])+1]+1/2 Log[(-1+Sqrt[4v^2+1])/(2v)]-1/2;
DiracLog2[pinf_,NN_, K_,mu_] := Module[{Mat,ret,nu,sdata,dp,Voff,idex,p, iu,iv},
        dp = pinf/NN;
        sdata={};
        nu=Sqrt[2 mu]//N;
        Voff=-P[mu]//N;

        For[idex=2,idex<=NN-1,idex=idex+1,
                p = idex dp;
                iv = idex;
                iu = idex+NN;
                sdata = Join[sdata,{{iv,iu+1} -> nu/(2.0 dp), {iv,iu-1} -> -nu/(2.0 dp), {iv,iu} ->nu K/p,
                        {iv,iv} -> ( Log[p] + mu  +Voff)}];
                sdata = Join[sdata,{{iu,iv+1} -> -nu/(2.0 dp), {iu,iv-1} -> nu/(2.0 dp), {iu,iv} ->nu K/p,
                        {iu,iu} ->(Log[p] - mu  +Voff)}];
        ];

        idex=1;
        iv = idex;
        iu = idex+NN;
        p = idex dp;
        sdata = Join[sdata,{{iv,iu+1} -> nu/( 2.0dp), {iv,iu} ->nu K/p,
                {iv,iv} ->  (Log[p] + mu +Voff)}];
        sdata = Join[sdata,{{iu,iv+1} -> -nu/(2.0 dp), {iu,iv} -> nu K/p,
                 {iu,iu} ->  ( Log[p] - mu +Voff)}];

        idex=NN;
        iv = idex;
        iu = idex+NN;
        p = idex dp;
```

```
31          sdata = Join[sdata,{ {iv,iu-1} -> -nu/(2.0 dp), {iv,iu} ->nu K/p,
32                  {iv,iv} ->  ( Log[p] + mu  +Voff)}];
33          sdata = Join[sdata,{{iu,iv-1} -> nu/(2.0 dp), {iu,iv} -> nu K/p,
34                  {iu,iu} ->  ( Log[p] - mu +Voff)}];
35
36          Mat =SparseArray[sdata]//N;
37          Return[Mat];
38  ]
```

References

[1] F. J. Asturias and S. R. Aragón, American Journal of Physics **53**, 893 (1985).

[2] P. A. Reiser, in *A symposium on two-dimensional science and technology*, edited by A. K. Dewdney (1981), pp. 61–73.

[3] J. Franklin and T. Garon, Physics Letters A **375**, 1391 (2011).

[4] D. J. Griffiths, *Introduction to Quantum Mechanics* (Pearson Education, 2006), 2nd ed.

[5] B. Zaslow and M. E. Zandler, American Journal of Physics **35**, 1118 (1967).

[6] A. M. Essin and D. J. Griffiths, American Journal of Physics **74**, 109 (2006).

[7] S.-H. Dong, Z.-Q. Ma, and G. Esposito, Foundations of Physics Letters **12**, 465 (1999).

[8] D. Ter Haar, *The Old Quantum Theory*, Selected Reading in Physics (Pergamon Press, 1967).

[9] P. Strange, *Relativistic Quantum Mechanics* (Cambridge University Press, 1998).

[10] S. R. Aragón, in *A symposium on two-dimensional science and technology*, edited by A. K. Dewdney (1981), pp. 99–117.

[11] G. H. Golub and C. F. Van Loan, *Matrix Computations* (Johns Hopkins University Press, 1996), 3rd ed.

[12] Y. Saad, *Iterative Methods for Sparse Linear Systems* (SIAM, 2003), 2nd ed.

[13] W. H. Press, S. A. Teukolsky, W. T. Vetterling, and B. P. Flannery, *Numerical Recipes* (Cambridge University Press, 2007), 3rd ed.

[14] M. M. Nieto, American Journal of Physics **47**, 1067 (1979).

[15] R. E. Moss, American Journal of Physics **55**, 397 (1987).